

## Short Communication

# Fabrication and Characterization of Visible Light active Fe-TiO<sub>2</sub> Nanocomposites as Nanophotocatalyst

M. Mirzaei, H. Ahadi, M. Shariaty-Niassar\* and M. Akbari

Transport Phenomena and Nano Technology (TPNT) laboratory, Dept. of Chem. Eng.,  
Faculty of Engineering, University of Tehran, Tehran, I. R. Iran

(\*) Corresponding author: mshariat@ut.ac.ir

(Received: 07 Feb 2014 and Accepted: 28 June 2015)

### **Abstract**

*In this research Fe-TiO<sub>2</sub> nanocomposites with different molar ratios of Fe/Ti were prepared as nano-photocatalyst using a modified Sol-Gel process at ambient temperature. Crystallographic properties of nanocomposites were characterized by X-ray Diffraction (XRD). Surface morphology and mean particle size of nanocomposites were specified by Field Emission Scanning Electron Microscopy (FESEM) and light absorption spectrum of nanocomposites was evaluated by Diffuse Reflectance Spectra (DRS). XRD patterns revealed that Fe<sup>3+</sup> is successfully substituted by Ti<sup>4+</sup> in TiO<sub>2</sub> lattice and no rutile phase is present in nanocomposites. From FESEM images it was specified that mean particle size of nanocomposites changed in the range of 28-47nm and narrow size distribution was seen. DRS analysis represented that by doping of Fe into the TiO<sub>2</sub> lattice, light absorption spectrum of TiO<sub>2</sub> shifted to visible light spectrum and led to decrement in energy band gap of TiO<sub>2</sub>. Band gap of nano-photocatalysts was in the range of 1.98-2.89 eV.*

**Keywords:** Sol-Gel, Nano-photocatalyst, Visible light

## 1. INTRODUCTION

Environmental pollution on a global scale is expected to be the greatest problem that chemical scientists will face in the 21<sup>st</sup> century. For this; an increasing number of researchers are looking for new photocatalytic systems to approach a solution (wade, 2005). During the last decades, metal oxide semiconductors have been widely considered all over the world for their high potential and excellent performance in photocatalytic applications (A. Fujishima, 2000; A. Fujishima, 2008; K. Hashimoto, 2005).

Existing photocatalytic systems are effective for the decomposition of many organic pollutants by the use of efficient corresponding semiconductors activated by ultra-violet (UV) irradiation (wade, 2005; H. Feng, 2012). The demand for such systems activated by visible light is rapidly increasing. The efficiency of activated

photocatalysts by the solar spectrum is severely limited (C.L. Yu, 2010; E. Piera, 2002). However, a new generation must be created to utilize the available solar spectrum. The most common nano photocatalyst is TiO<sub>2</sub>, offering good properties such as moderate band gap (3.2eV), non-toxicity, water insolubility, low cost, high surface area, environmental compatibility, superior chemical and photochemical stability and easy availability (wade, 2005; H. Feng, 2012; S. Luo, 2011; X. Lin, 2011). Titanium oxide is an important semiconductor material which is being used in a wide range of applications including photocatalysis, environmental pollution control, electronic industry and solar energy conversion (Kazuya Nakataa, 2012; Shuxi Dai, 2010; N.R. Khalid, 2013). Hence, the absorption peak of TiO<sub>2</sub> should be transmitted to the

visible waves. For this purpose, TiO<sub>2</sub> is modified by various means like coupling with a narrow band gap semiconductor, metal ion/nonmetal ion doping, co-doping with two or more foreign ions, surface sensitization by organic dyes or metal complex (A.Omo Ibadon, 2013). In this study, Fe<sup>3+</sup>-doped TiO<sub>2</sub> nanophotocatalysts were prepared using Sol-Gel method and characterized by X-ray Diffraction, Field Emission Scanning Electron Microscopy and Diffuse Reflectance Spectra.

## 2. MATERIALS AND METHOD

Titanium (IV) tetra isopropoxide (TTIP, 97% Aldrich) as precursor alkoxide for titanium, 1-Propanol (99.5% Merck) as solvent to control the ions movement in reaction media, iron nitrate nonahydrate (Fe(NO<sub>3</sub>)<sub>3</sub>.9H<sub>2</sub>O, 99% Merck) as precursor for Fe<sup>3+</sup> ions in Fe-TiO<sub>2</sub> nanocomposite, distilled water, nitric acid (HNO<sub>3</sub>, 65% Merck) and sodium hydroxide (NaOH ≥ 97% Merck) as catalysts for hydrolysis reaction were all used without additional purification.

### 2.1. Nano-photocatalyst preparation

Photocatalysts were prepared using modified Sol-Gel method based on the operational conditions shown in table 1.

In all the experiments, specific trend of Fe-TiO<sub>2</sub> nanophotocatalysts preparation was followed (Figure. 1). At the first stage (Figure.1 (a)) 15cc TTIP as alkoxide precursor was dissolved completely in 45cc 1-propanol (formation of solution A) which is an appropriate solvent for sol-gel process; that is due to its low dielectric point comparing with water.

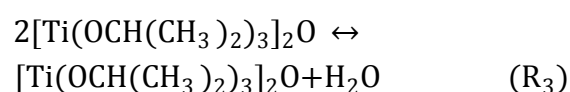
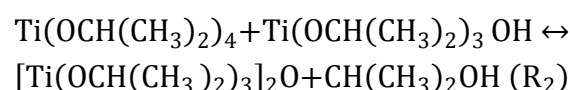
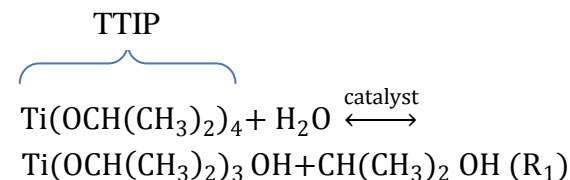
**Table 1.** operational conditions for synthesis of nano photocatalysts

Sample	Fe/Ti (molar)	T <sub>c</sub> (° C) <sup>1</sup>	t <sub>ca.</sub> (hr.) <sup>2</sup>	pH
a	0.001	600	4	1
b	0.0255	500	3	6.5
c	0.05	400	4	1

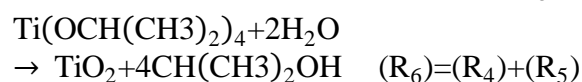
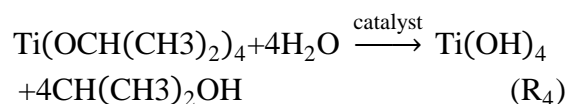
<sup>1</sup> calcination temperature

<sup>2</sup> calcination time

Then from molar ratio of Fe to Ti, required Fe(NO<sub>3</sub>)<sub>3</sub>.9H<sub>2</sub>O was determined and then dissolved in water (formation of solution B). Reaction mechanism of sol- gel process is as follows:



Another general reaction mechanism for synthesis of TiO<sub>2</sub> is:



According to stoichiometry of sol-gel reaction (R<sub>4</sub>) the molar ratio of water to TTIP is 2. At the second stage (Fig.1 (b)) solution A was added drop wise into the solution B while the mixture was agitating rigorously on a magnetic stirrer with 750 rpm at ambient temperature (20±1°C). In order to control the pH of mixture, Metrohm827 pH meter was used. HNO<sub>3</sub> or NaOH was then gradually added under vigorous stirring as a catalyst for hydrolysis reaction of TTIP (R<sub>1</sub> or R<sub>4</sub>).

During the mixing, colloidal, slurry and stable sol was formed and up to 24hours after sol formation the gel was formed due to the condensation reaction (R<sub>2</sub> & R<sub>3</sub>). For aging purposes, the prepared gel was kept for one day (i.e. aging time). At the third stage (Fig.1(c)) the gel was washed away

with distilled water and centrifuged at 4000 rpm for several times to remove the impurities such as  $\text{Na}^+$ ,  $\text{H}^+$  and  $\text{OH}^-$  ions until its pH was equal to that of distilled water (pH=7). Then, the gel was again washed with alcohol two or three times to remove water. That is due to the high solubility of alcohol in water. The solvent (i.e. 1-propanol) was also used for gel washing to prevent particle growth due to hydrogen bond formation in the presence of water in the gel. For initial drying, washed gel was put in oven (Memmert D06836) for 24 hours at  $120^\circ\text{C}$ . The resulting hunk was properly crushed and

put in a high temperature electrical furnace (Exciton, EX.1200-12L) for calcination operations with a thermal time gradient of  $5^\circ\text{C}/\text{min}$ .

### 3. RESULT AND DISCUSSION

X-ray Diffraction (XRD) was carried out using X-ray diffractometer (X' pert Philips,  $\text{Cu K}\alpha$  irradiation,  $\lambda=1.54056^\circ\text{A}$  and a voltage and current of 40 Kv and 30 mA) to identify the crystallographic properties such as phase structure, average crystallite size, relative crystallinity and chemical composition.

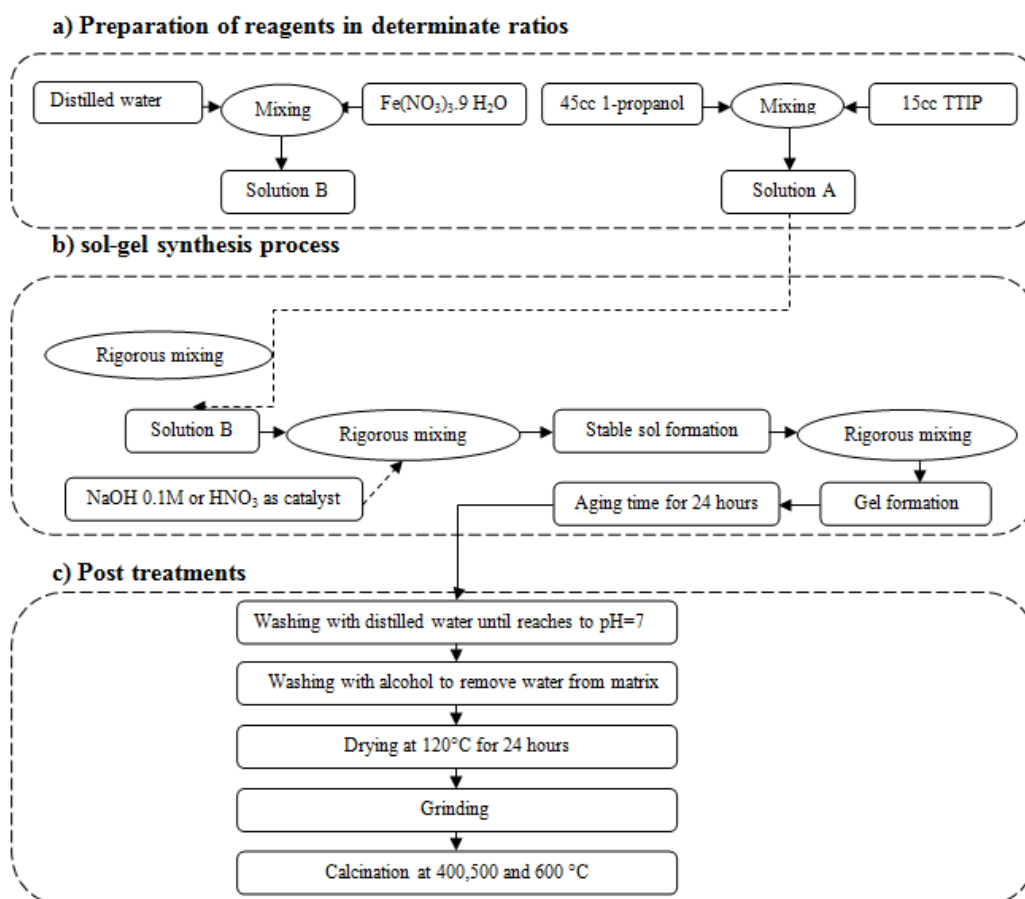


**Figure 1.** Flow chart for fabrication of  $\text{Fe-TiO}_2$  nanocomposites by sol-gel method

Modified sol-gel method revealed tetragonal crystalline system for titanium dioxide in anatase phase structure (JCPDS No. 01-073-1764). As expected in all patterns, sharp peaks of  $\text{Fe}_2\text{O}_3$  were not detectable due to its low concentration, small crystallite size or amorphous

crystalline system. In all the crystalline patterns, sharp peaks was detected at  $2\theta=25.4^\circ, 38^\circ, 48^\circ, 54^\circ, 62^\circ$  and  $75^\circ$  for anatase phase structure of  $\text{TiO}_2$  corresponded to (101) crystalline plane. Sharp peaks signify good crystallinity of nanoparticles and approve that  $\text{TiO}_2$  crystals were

successfully formed. XRD diagrams represent that by Fe doping into the crystal lattice of anatase  $\text{TiO}_2$ , characteristic sharp peak of 101 plane has been shifted to low angles. It implies that  $\text{Fe}^{3+}$  has been successfully substituted by  $\text{Ti}^{4+}$  into the  $\text{TiO}_2$  lattice. Mean crystallite size of anatase  $\text{TiO}_2$  crystallites calculated by Scherrer algorithm from broadening of (101) plane reflection was in the range of 20-40 nm. Fig.2 shows XRD patterns for Fe- $\text{TiO}_2$  nanophotocatalysts.

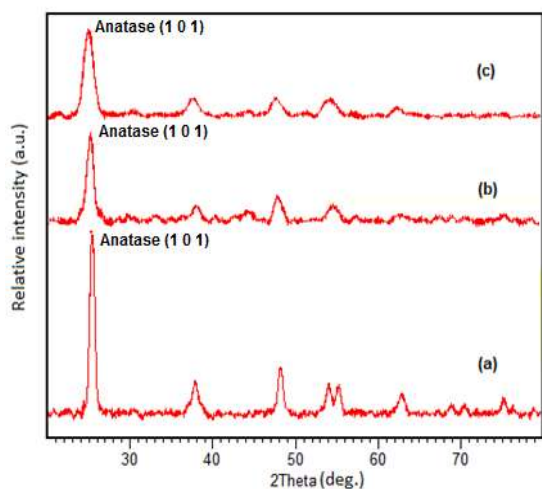


**Figure2.** XRD patterns for Fe- $\text{TiO}_2$  nanophotocatalysts

For calculation of mean particle size, FESEM images were analyzed by Microstructure Measurement software together with statistical methods. Accuracy of mean particle size with 95% confidence interval was determined by t-test (which is a statistical method). Mean particle size of synthesized nanopowders was in the range of 28–47 nm. Figure.3 represents the FESEM images of nanophotocatalysts.

Figure.4 shows Diffuse Reflectance Spectra (DRS) analysis of samples. 0.1% mole fraction Fe- $\text{TiO}_2$  (sample (a)) was characterized with a sharp absorption edge at about 425nm (energy band gap~2.89eV). 2.55% mole fraction Fe- $\text{TiO}_2$  (sample (b)) showed relatively more extended absorption spectra into the visible-light region at absorption edge about 458nm (energy band gap~2.71eV).

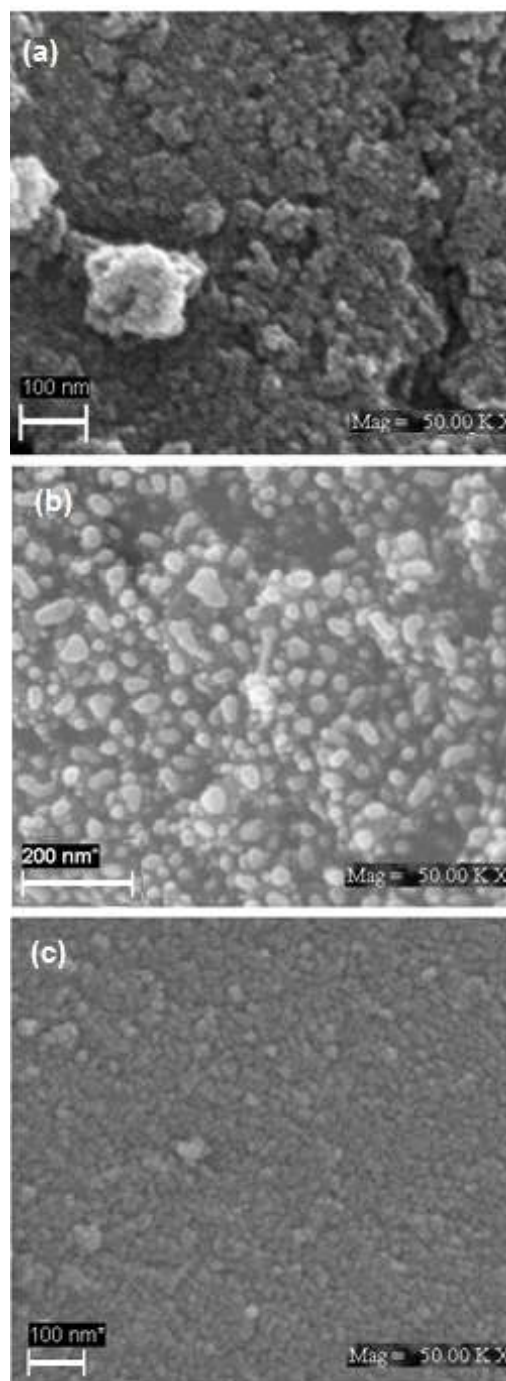


**Figure3.** FESEM images of Fe- $\text{TiO}_2$  nanophotocatalysts

5% mole fraction Fe- $\text{TiO}_2$  exhibited substantial and broad absorption shoulders up to 625 nm (energy band gap~1.98eV). The extended absorption spectra of Fe- $\text{TiO}_2$  into visible-light region were achieved by improvement of electronic energy band structure of  $\text{TiO}_2$  through doping  $\text{Fe}^{3+}$  metal ions. The enhanced absorption of Fe- $\text{TiO}_2$  in visible light region is because of the excitation of 3d

orbital electrons of doping Fe ions to the conduction band of TiO<sub>2</sub> according to their respective energy levels.

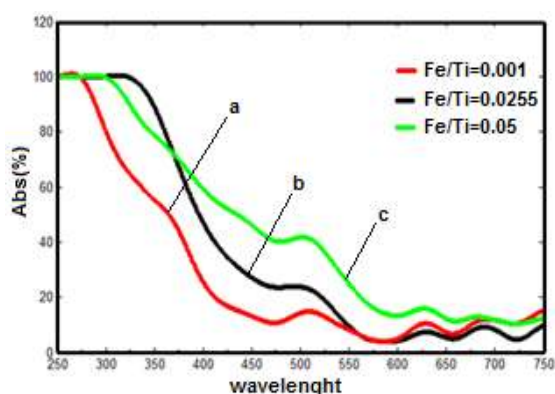


**Figure 4.** Diffuse reflectance spectra of prepared Fe-TiO<sub>2</sub> nanophotocatalysts

#### 4. CONCLUSION

Fe-TiO<sub>2</sub> nano photocatalysts were successfully synthesized using modified Sol-Gel process. They had good crystalline structure, high crystallinity, narrow size distribution and mean particle size in the range of 28-47nm. There was no rutile phase in nanoparticles and only anatase phase was present. It was specified that by Fe-doping into TiO<sub>2</sub> lattice, light absorption spectrum of nanoparticles was shifted to visible light region. Increment of Fe/Ti molar ratio from 0.001 to 0.05, led to decrease in energy band gap from 2.89 to 1.98; so they are appropriate to use in photocatalysis process.

#### REFERENCES

1. Fujishima, A., Rao, Tryk, D.A. (2000). "Titanium dioxide photocatalysis", *Journal of Photochemistry and Photobiology C*, 1, 1-12.
2. Fujishima, A., Zhang, X. & Tryk, D.A. (2008). "TiO<sub>2</sub> photocatalysis and related surface phenomena", *Journal of Surface Science Reports*, 63: 515-582.
3. Omo Ibadon, A., Fitzpatrick, P.(2013). "Heterogeneous Photocatalysis: Recent Advances and Applications", *Journal of Catalysts*, 3: 189-218.
4. Yu, C.L., Cai, D.J., Yang, K., Yu, J.C., Zhou, Y., Fan, C. F.(2010). "Sol-Gel Derived S,I-Codoped Mesoporous TiO<sub>2</sub> Photocatalyst with High Visible-Light Photocatalytic Activity", *Journal of Physics and Chemistry of Solids*, 71: 1337-1343.
5. Piera, E., Ayllon, J. A., Domenech, X.& Peral, J. (2002). "TiO<sub>2</sub> Deactivation During Gas-Phase Photocatalytic Oxidation of Ethanol", *Journal of Catalysis Today*, 76: 259-270.
6. Feng, H., Zhang, M. H. & Yu, L. E.(2012). "Hydrothermal Synthesis and Photocatalytic Performance of Metal-Ions Doped TiO<sub>2</sub>", *Journal of Applied Catalysis A: General*, 413-414: 238-244.
7. Hashimoto, K., Irie, H.& Fujishima, A. (2005). "TiO<sub>2</sub> photocatalysis: a historical overview and future prospects", *Journal of Applied Physics*, 44: 8269-8285.
8. Nakataa, K., Fujishima, A. (2012)."TiO<sub>2</sub> photocatalysis: Design and applications", *Journal of Photochemistry and Photobiology C: Photochemistry Reviews*, 13: 169-189.
9. Khalid, N.R., Ahmed, E., Hong, Z., Zhang, Y., Ullah, M.& Ahmed, M.(2013). "Graphene modified Nd/TiO<sub>2</sub> photocatalyst for methyl orange degradation under visible light irradiation", *Journal of Ceramics International*, 39: 3569-3575.
10. Luo, S., Xiao, Y., Yang, L., Liu, C., Su, F., Li, Y., Cai, Q.& Zeng, G.(2011). "Simultaneous detoxification of hexavalent chromium and acid orange 7 by a novel Au/TiO<sub>2</sub> heterojunction composite nanotube arrays", *Journal of Separation and Purification Technology*, 79: 85-91.
11. Dai,S., Wu, Y., Sakai, T., Du, Z. , Sakai, H.& Abe, M.(2010). "Preparation of highly crystalline TiO<sub>2</sub> nanostructures by acid-assisted hydrothermal treatment of hexagonal structured nanocrystalline Titania/Cetyltrimethylammonium bromide nano skeleton", *Journal of Nanoscale Research Letters*, 5: 1829-1835.
12. Wade, J. (2005). "An Investigation of TiO<sub>2</sub>-ZnFe<sub>2</sub>O<sub>4</sub> Nanocomposites for Visible Light Photocatalysis in Electrical Engineering", A Thesis Submitted to Department of Electrical Engineering, University of South Florida, USA.
13. Lin, X. , Rong, F., Fu, D., Yuan, C. (2011). "Enhanced photocatalytic activity of fluorine doped TiO<sub>2</sub> by loaded with Ag for degradation of organic pollutants", *Journal of Powder Technology*, 219: 173-178.